Available online at www.sciencedirect.com
SCIENCE DIRECT®
Journal of Pharmaceutical and Biomedical Analysis
34 (2004) 53–66
JOURNAL OF PHARMACEUTICAL AND BIOMEDICAL ANALYSIS
www.elsevier.com/locate/jpba

API-ionspray MS and MS/MS study on the structural characterization of bisbenzylisoquinoline alkaloids

Wu-Nan Wu*, Michael D. Moyer

The Division of Drug Evaluation, Johnson and Johnson Pharmaceutical Research and Development, L.L.C., Spring House, PA 19477, USA

Received 20 October 2002; received in revised form 20 June 2003; accepted 16 August 2003

Abstract

API-ionspray MS and MS/MS techniques have been utilized to elucidate the structures of 20 bisbenzylisoquinoline alkaloids, consisting of 17 diether and three monoether links of two benzyltetrahydroisoquinoline units, which were isolated and identified previously from a variety of *Thalictrum* sp. (Ranunculaceae family). Apparent protonated molecular ions ($[M + H]^+$) and very intense doubly-protonated molecular ion ($[M + 2H]^{++}$, 100% of relative abundance) in Q1 Scan MS spectra and prominent as well as diagnostic product ions for the structural information in MS/MS spectra were observed in nanogram quantities for all investigated alkaloids.

Keywords: API-ionspray; MS and MS/MS; Bisbenzylisoquinoline alkaloids; Thalictrum sp.; Structural characterization

1. Introduction

The families of Anonaceae, Berberidaceae, Hernandiaceae, Lauraceae, Magnoliaceae, Menispermaceae, Monimiaceae, Nymphaceae, Ranunculaceae, Rutaceae, and Papaveraceae, contain a homodimeric classes of several hundred members of the so-called bisbenzylisoquinoline alkaloids, which are derived biogenetically via phenol-oxidative coupling of two units of benzyltetrahydroisoquinoline alkakloids. Bisbenzylisoquinoline alkaloids exert hypotensive, antimicrobial, analgesic, muscle relaxant, and antitumor activities [1–5]. Obamegine, thalrugosine, thalrugosidine, and thalistyline of the 20 investigated alkaloids exhibit antimicrobial and hypotensive activity [1–5]. Previously, structural elucidation of these natural products have mainly relied on EI-MS, CI-MS and FAB-MS, however, these techniques are not sensitive, and need more than 10 μg of material [4,6–22]. Early EI-MS and FAB-MS studies displayed low abundances of molecular/adduct molecular ions and fragment ions for these alkaloids [4,6–22]. CI-MS showed intense protonated molecular ions for these secondary and tertiary alkaloids with very less fragment ions for the structural information of the secondary and tertiary alkaloids, and no molecular ions detected for the quaternary alkaloids [4,6–22]. We have reported previously preliminary results for the structural fragments from these 20 monoether and diether links of bisbenzylisoquinoline alkaloids using API-ionspray MS and MS/MS techniques [23]. This paper describes in detail for the structural character-

* Corresponding author. Tel.: +1-215-6285562; fax: +1-215-6287822.
E-mail address: wwu@prius.jnj.com (W.-N. Wu).

0731-7085/$ – see front matter © 2003 Elsevier B.V. All rights reserved.
doi:10.1016/j.japna.2003.06.002

ization of different classes of bisbenzylisoquinoline alkaloids each in ng quantities using API-ionspray MS and MS/MS techniques.

2. Experimental

2.1. Materials

A total of 20 investigated bisbenzylisoquinoline alkaloids consisting of seventeen diether and three monoether linkes of two benzyltetrahydroisoquinoline units, were previously isolated from *Thalictrum* species (Ranunculaceae) indigenous in the United States and Colombia [15–22].

HPLC-grade solvents were purchased from the Fisher Scientific Co. (Fairlawn, NJ, USA) and glass-distilled solvents were obtained from Burdick and Jackson Laboratories Inc. (Muskegon, MI, USA).

2.2. Sample analysis

Twenty alkaloids were each reconstituted in acetonitrile–water (50/50, v/v, with 2 mM ammonium acetate buffer, pH 4.0) to a concentration of 50 ng/μl and then analyzed 5–15 μl of sample solutions via 20 μl flow-injector using the PE Sciex API III-Plus MS (Perkin-Elmer Sciex Instruments, Thornhill, Ontario, Canada), a triple quadrupole mass spectrometer, interfaced to a Hitachi HPLC solvent delivery system (L-6200 A Intelligent pump) via an ionsprayer using nitrogen as a curtain and nebulizing gas and argon as a collision gas for MS/MS analysis. All API-ionspray mass spectra in positive-ion mode were acquired using the following conditions: ionspray voltage—5.5 kV; orifice voltage—55 V; scan range—*m*/*z* 50–1000; collision energy for product ions-20 eV; collision gas thickness—240 × 10^{13} molecules/cm; curtain gas (N2) set—10. The mobile phase for this system was the same buffer as described for the alkaloids reconstitution, at a flow rate of 0.1 ml/min.

3. Results and discussion

Biological activities of the 20 bisbenzylisoquinoline alkaloids have been investigated previously [1–5, 15–21]. Among them, thalugosine, thalugosidine, thalrugosaminine, thalidezine, thalistyline, hernandezine and *O*-methyl thalicberine exhibited antimicrobial activity against *Mycobacterium smegmatis* [3,4,15–18], and obamegine, isotetrandrine, thalrugosaminine, thalidasine and thalistyline showed hypotensive activity in the dog and rabbit [4,16–18].

Twenty bisbenzylisoquinoline alkaloids consisting two groups, group A (compounds #1–17) with 17 diether linkes by two benzyltetrahydroisoquinoline units and group B (compounds #18–20) with three monoether linkes by two benzyltetrahydroisoquinoline units (rings ABE and rings CDE) (Fig. 1) were studied. Of the17 diether-linked alkaloids, #1–3, are *S* and *R* configuration, #4–6, *R* and *S* configuration and #7–17, are *S* and *S* configuration [1,2,4]. All of three monoether-linked alkaloids, compounds #18–20 are *S* and *S* configuration [1,2,4]. All of bisbenzylisoquinoline alkaloids exhibited intense protonated molecular ions ($[M + H]^+$), along with the doubly-protonated molecular ions ($[M + 2H]^{++}$) with 100% relative abundance (r.a.) in the Q1 scan MS with the exception of thalicberine, which showed a 100% (r.a.) protonated molecular ion with a doubly-protonated molecular ion (36%, r.a.). The MS and MS/MS analysis of each alkaloid revealed the prominent as well as diagnostic products ions for the structural elucidation. The structures of 20 investigated bisbenzylisoquinoline alkaloids (Fig. 1), their important product ions, and the representative Q1 scan MS and MS/MS spectra (Figs. 2–6) are illustrated.

Obamegine (Fig. 1; compound #1), $C_{36}H_{38}O_6N_2$ (MW: 594), showed an intense protonated molecular ion at *m*/*z* 595 (17%, r.a.) with a doubly-protonated molecular ion at *m*/*z* 298 (100%, r.a.) in the Q1 scan MS spectrum. The MS/MS spectrum displayed product ions at *m*/*z* (%, r.a.) 579 ($[M + H]^+$–CH_4, 2), 564 (9), 532 (18), 382 (**a**, 4), 381 (**a**-H, 2), 367 (**b**, 92), 351 (5), 339 (**b**-CO, 3), 213 (**g**, 5), 192 (**f**, 100), 191 (**f**-H, 40), 176 (24), 174 (21), and 148 (9), along with an apparent protonated molecular ion at *m*/*z* 595 (16) (Fig. 6).

Thalrugosine (Fig. 1; compound #2), $C_{37}H_{40}O_6N_2$ (MW: 608), revealed an intense protonated molecular ion at *m*/*z* 609 (44%, r.a.), together with a doubly-protonated molecular ion at *m*/*z* 305 (100%, r.a.) in the Q1 scan MS data (Fig. 2). The MS/MS data showed important product ions at *m*/*z* (%, r.a.) 591 ($[M+H]^+$-H_2O, 3), 578 ($[M+H]^+$-OMe,16), 566 (18), 546 (21),

382 (**a**, 10), 381 (**a**-H, 9), 367 (**b**,100), 351 (**b**-CH_4, 7), 336 (4), 280 (5), 227 (**h**, 6), 192 (**f**, 49), 177 (7), 176 (**f**-CH_4, 23), 174 (**f**-H_2O, 24), and 146 (13) with a protonated molecular ion at *m/z* 609 (43) (Figs. 2 and 6).

Isotetrandrine (Fig. 1; compound #3), $C_{38}H_{42}O_6N_2$ (MW: 622), exhibited an intense protonated molecular ion at *m/z* 623 (31%, r.a.) with a doubly-protonated molecular ion at *m/z* 312 (100%, r.a.) in the Q1 scan MS. The MS/MS analysis gave fragment product ions at *m/z* (%, r.a.) 607 ($[M+H]^+$-CH_4, 7), 592 ($[M+H]^+$-OMe, 6), 576 (592-CH_4, 9), 560 (9), 396 (**c**, 2), 395 (**c**-H, 2), 381 (**d**, 51), 363 (**d**-H_2O, 8), 335 (9), 294 (11), 227 (**h**,11), 206 (**e**, 8), 204 (14), 192 (**f**, 20), 191 (**f**-H, 24), 190 (**f**-2H, 31), 174 (**f**-H_2O, 100), 162

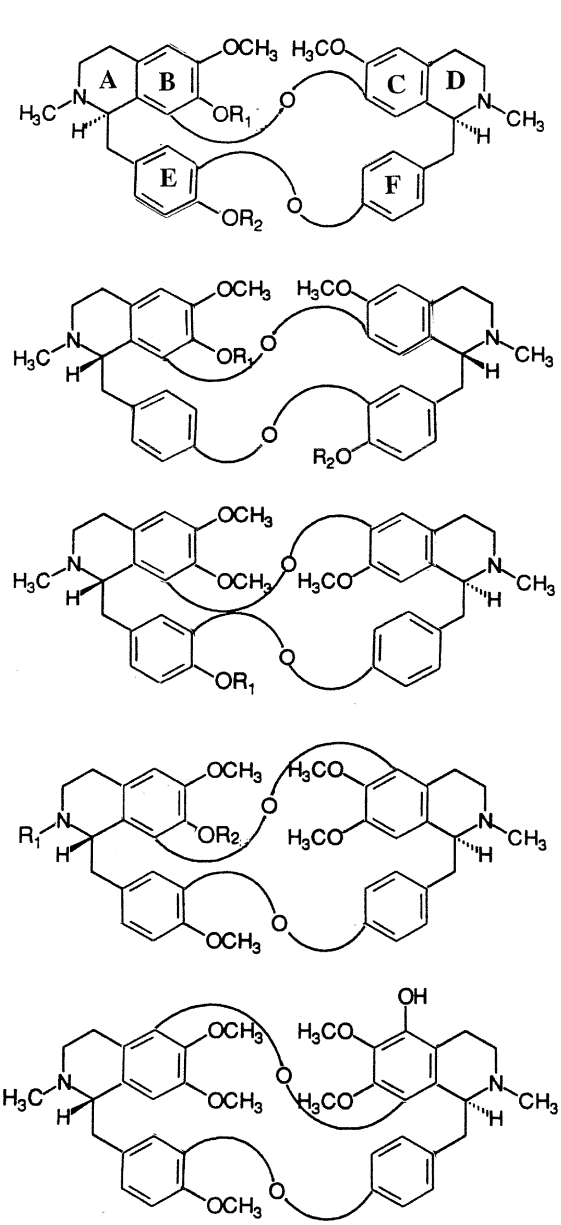

Group A

Compound	R_1	R_2
1. Obamegine	H	H
2. Thalrugosine	H	CH_3
3. Isotetrandrine	CH_3	CH_3
4. Homoaromoline	H	CH_3
5. Oxyacanthine	CH_3	H
6. Obaberine	CH_3	CH_3
7. Thalicberine	H	
8. O-Methyl thalicberine	CH_3	
9. Northalrugosidine	H	H
10. Thalrugosidine	CH_3	H
11. Thalidasine	CH_3	CH_3
12. Thalmirabine		

Fig. 1. Structures of 20 bisbenzylisoquinoline alkaloids.

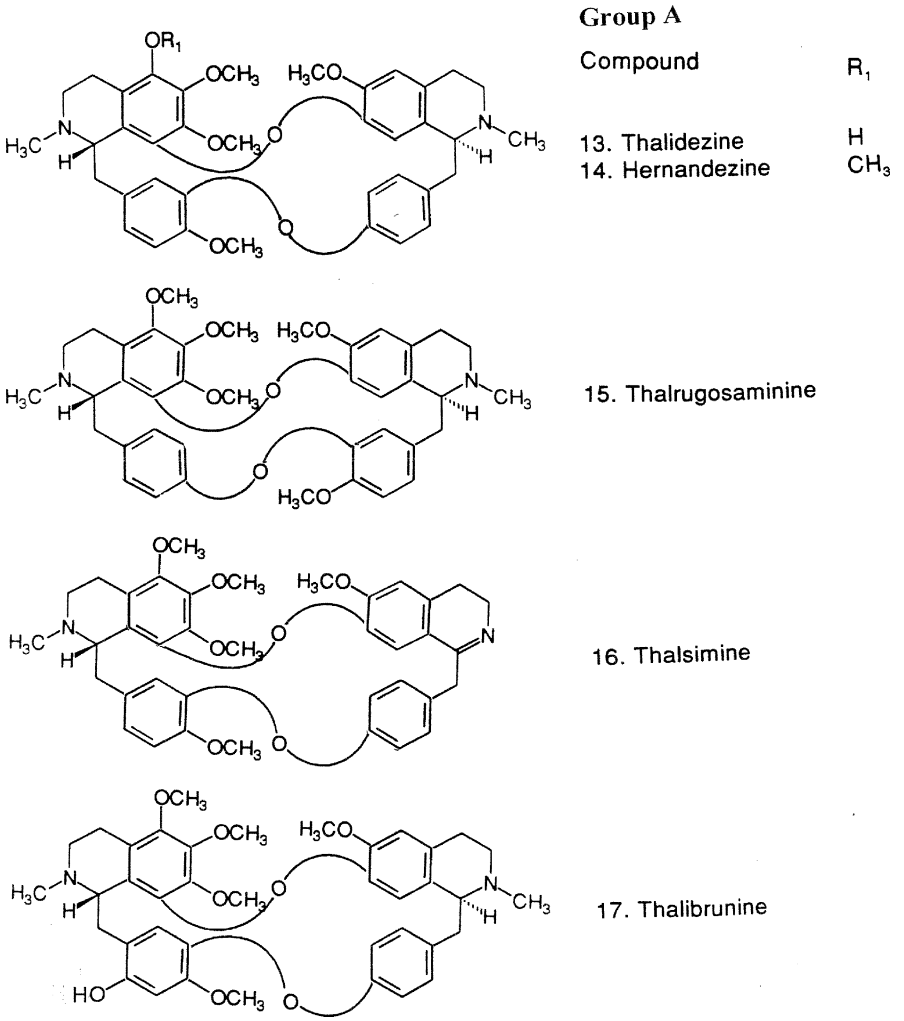

Fig. 1. (*Continued*)

(35), and 146 (38), together with an intense protonated molecular ion at *m*/*z* 623 (10) (Fig. 6).

Homoaromoline (Fig. 1; compound #4), $C_{37}H_{40}O_6N_2$ (MW: 608), displayed an apparent protonated molecular ion at *m*/*z* 609 (39%, r.a.), accompanying with a very intense doubly-protonated molecular ion at *m*/*z* 305 (100%, r.a.) in the Q1 scan spectrum MS. The MS/MS spectrum indicated diagnostic product ions at *m*/*z* (%, r.a.) 593 ($[M + H]^+$-CH_4, 5), 578 ($[M + H]^+$-OMe, 34), 566 (35), 535 (20), 520 (14), 400 (18), 385 (15), 382 (**a**, 9), 381 (**a**-H, 8), 367 (**b**, 100), 358 (22), 350 (14), 340 (12), 266 (27), 239 (24), 227 (**h**, 43), 213 (**h**-CH_2, 38), 192 (**f**, 8), 190 (**f**-2H, 64), 176 (**f**-CH_4, 78), and 146 (24) with a protonated molecular ion at *m*/*z* 609 (38) (Fig. 6).

Oxyacanthine (Fig. 1; compound #5), $C_{37}H_{40}O_6N_2$ (MW: 608), provided an apparent protonated molecular ion at *m*/*z* 609 (43%, r.a.), along with an intense doubly-protonated molecular ion at *m*/*z* 305 (100%, r.a.) in the Q1 scan MS spectrum. The MS/MS analysis of the protonated molecular ion revealed important product ions at *m*/*z* (%, r.a.) 593 ($[M + H]^+$-CH_4, 5), 578 ($[M+H]^+$-OMe, 36), 535 (20), 396 (**c**, 7), 395 (**c**-H, 6), 387 (18), 381 (**b**, 100), 367 (**b**-CH_2, 58), 213 (**g**, 42), 206 (**e**, 41), 192 (**f**, 61), and 176 (**f**-CH_4, 92), with a protonated molecular ion at *m*/*z* 609 (45) (Fig. 6).

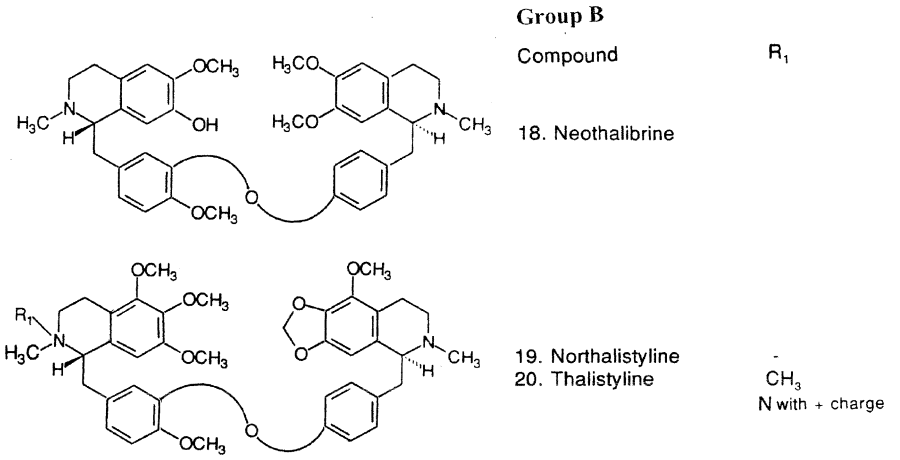

Fig. 1. (*Continued*).

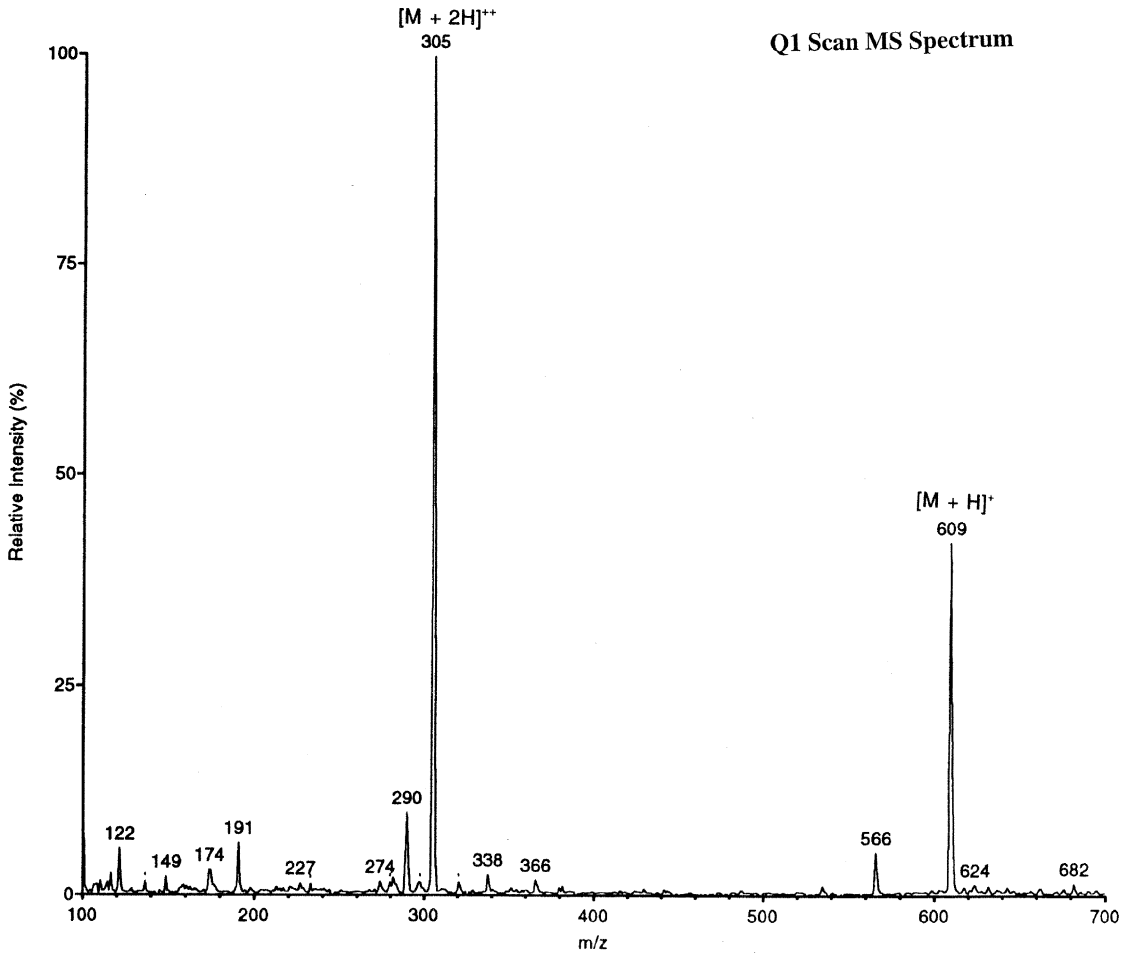

Fig. 2. API-Ionspray Q1 scan MS and MS/MS spectra of thalrugosine.

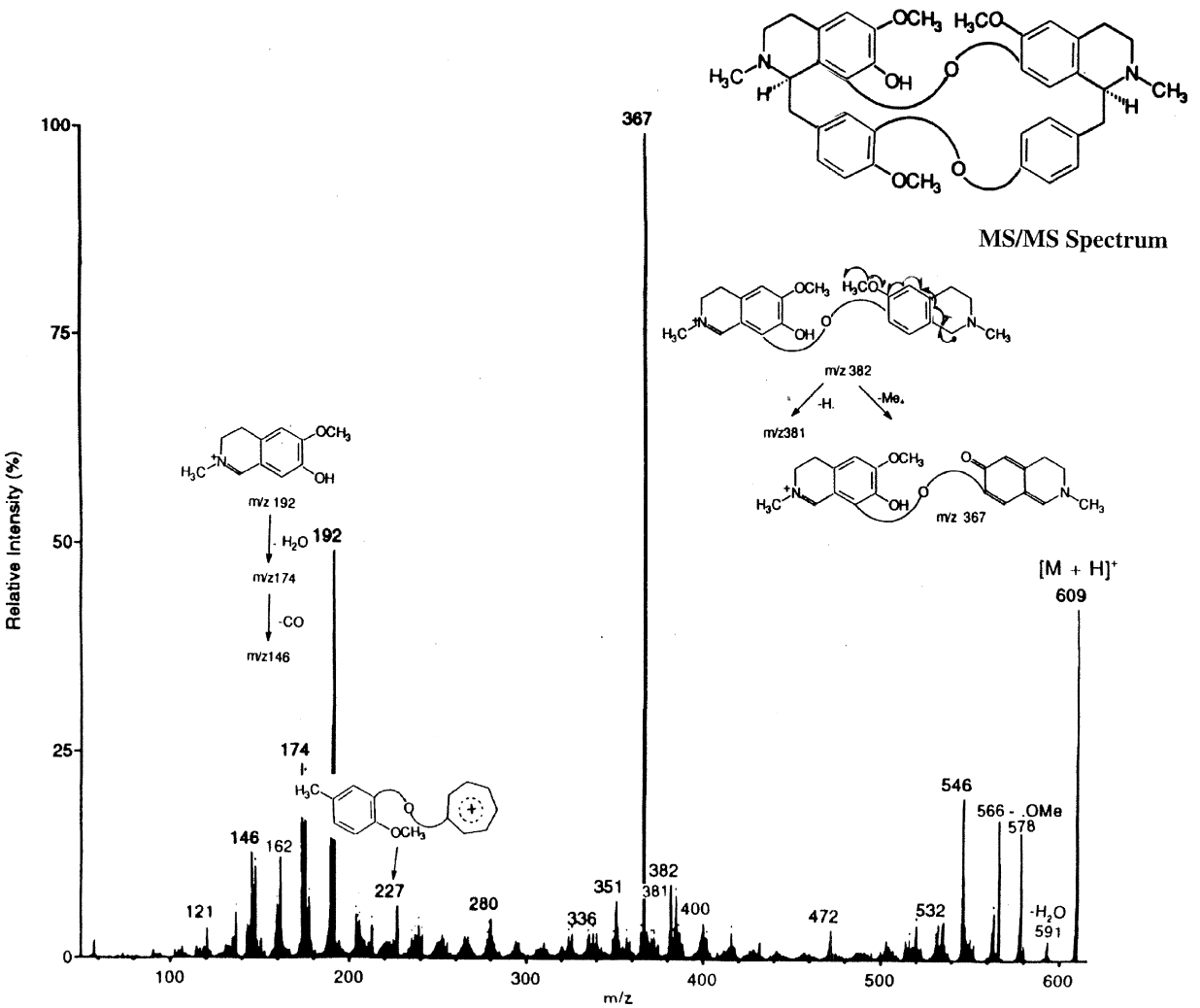

Fig. 2. (*Continued*).

Obaberine (Fig. 1; compound #6), $C_{38}H_{42}O_6N_2$ (MW: 622), gave an apparent protonated molecular ion at *m*/*z* 623 (24%, r.a.) with a doubly-protonated molecular ion at *m*/*z* 312 (100%, r.a.) in the Q1 scan MS data. The MS/MS data of this alkaloid exhibited product ions at *m*/*z* (%, r.a.) 607 ($[M + H]^+$-CH_4, 4), 592 (607-Me, 17), 580 (18), 400 (17), 396 (**c**, 5), 395 (**c**-H, 3), 381 (**d**, 100), 365 (**d**-CH_4, 12), 280 (12), 227 (**h**, 27), 206 (**e**, 25), 192 (**f**, 10), 190 (**f**-2H, 26), 176 (**f**-CH_4, 49), and 174 (**f**-H_2O, 57), with a protonated molecular ion at *m*/*z* 623 (24) (Fig. 6).

Thalicberine (Fig. 1; compound #7), $C_{37}H_{40}O_6N_2$ (MW: 608), showed a very intense protonated molecular ion at *m*/*z* 609 (100%, r.a.), together with an apparent doubly-protonated molecular ion at *m*/*z* 305 (36%, r.a.), and the MS/MS product ions displayed at *m*/*z* (%, r.a.) 592 ($[M + H]^+$-NH_3, 2), 578 ($[M + H]^+$-OMe, 29), 566 (14), 396 (**i**,12), 387 (28), 381 (**j**, 24), 367 (**j**-CH_2, 11), 280 (13), 222 (**k**, 24), 213 (**g**, 14), 206 (**e**, 28), 192 (**f**, 100), 176 (**f**-CH_4, 65), 174 (**f**-H_2O, 44), and 159 (39), along with a protonated molecular ion at *m*/*z* 609 (90) (Fig. 6).

O-Methyl thalicberine (Fig. 1; compound #8), $C_{38}H_{42}O_6N_2$ (MW: 622), exhibited an intense protonated molecular ion at *m*/*z* 623 and a doubly-protonated molecular ion at *m*/*z* 312 (100%, r.a.) in the

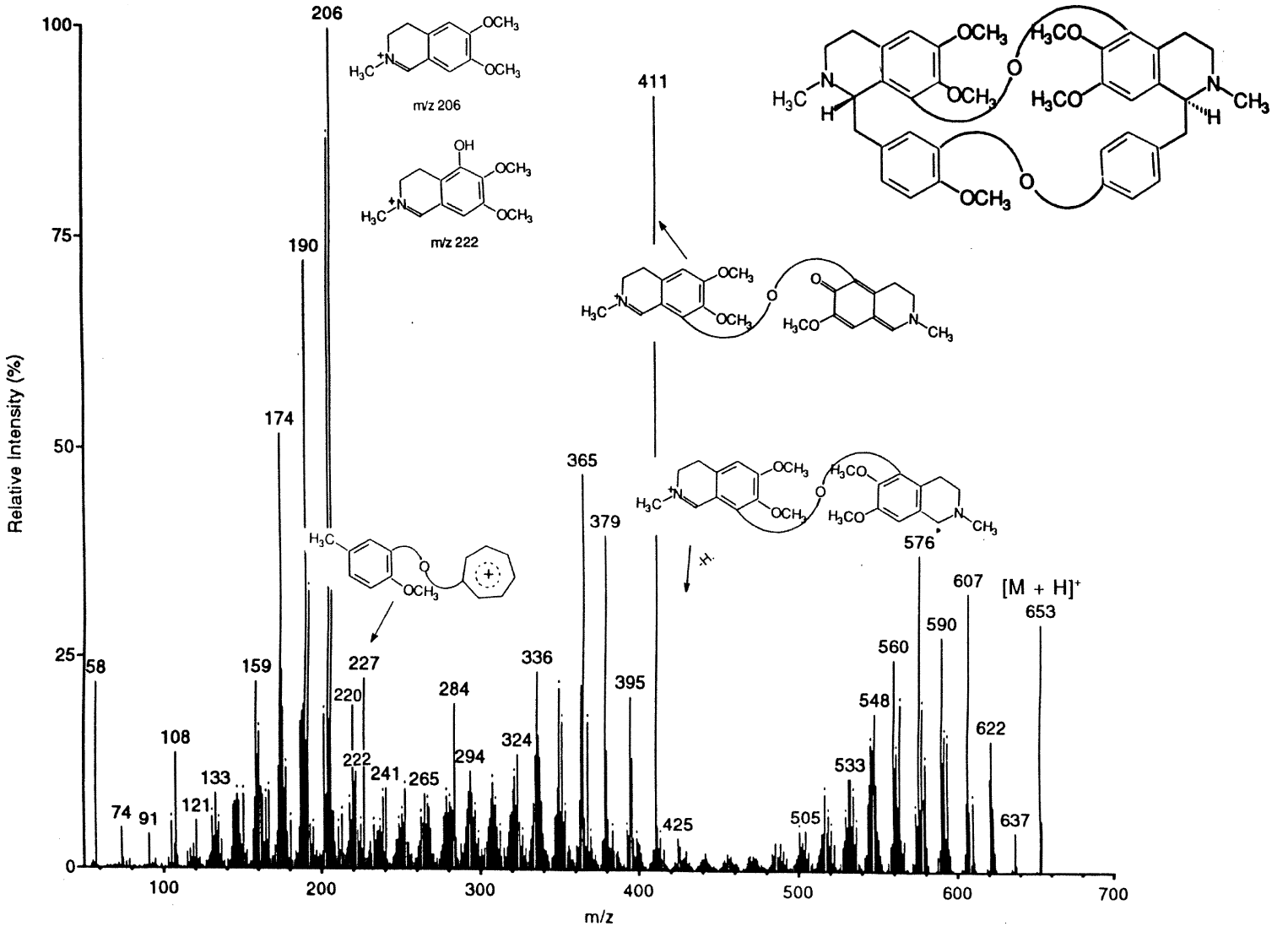

Fig. 3. API-Ionspray MS/MS spectrum of thalidasine.

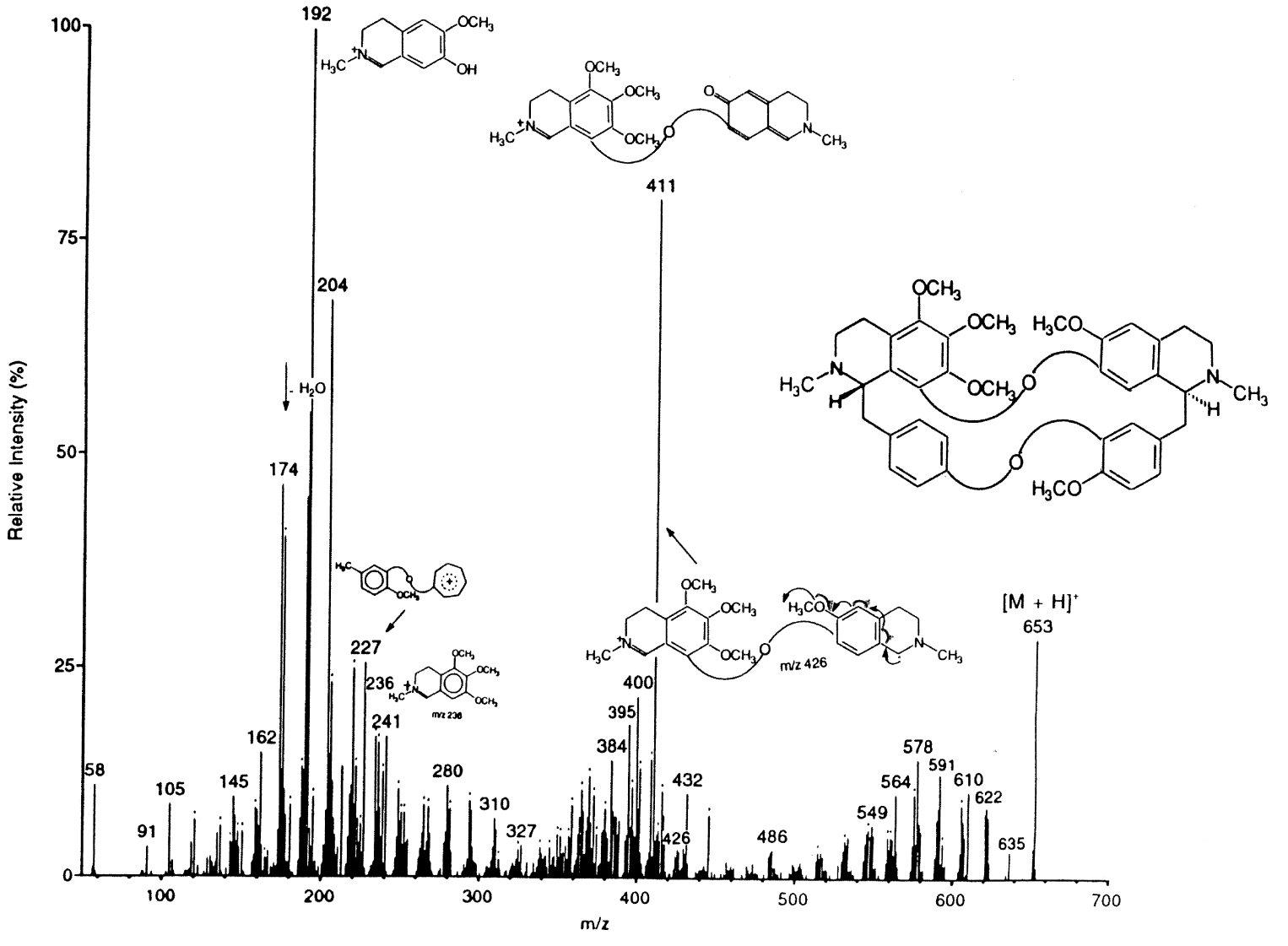

Fig. 4. API-Ionspray MS/MS spectrum of thalrugosaminine.

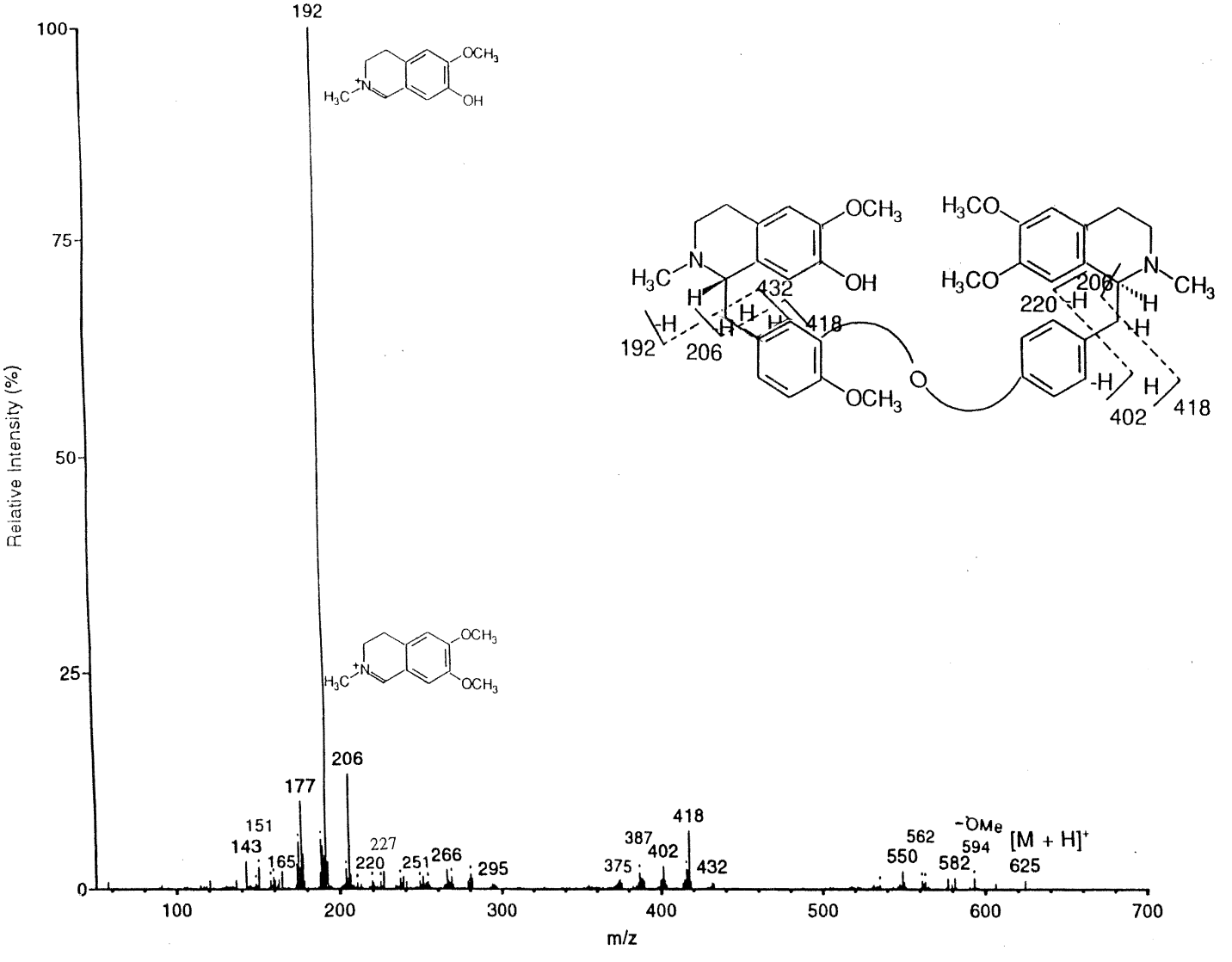

Fig. 5. API-Ionspray MS/MS spectrum of neothalibrine.

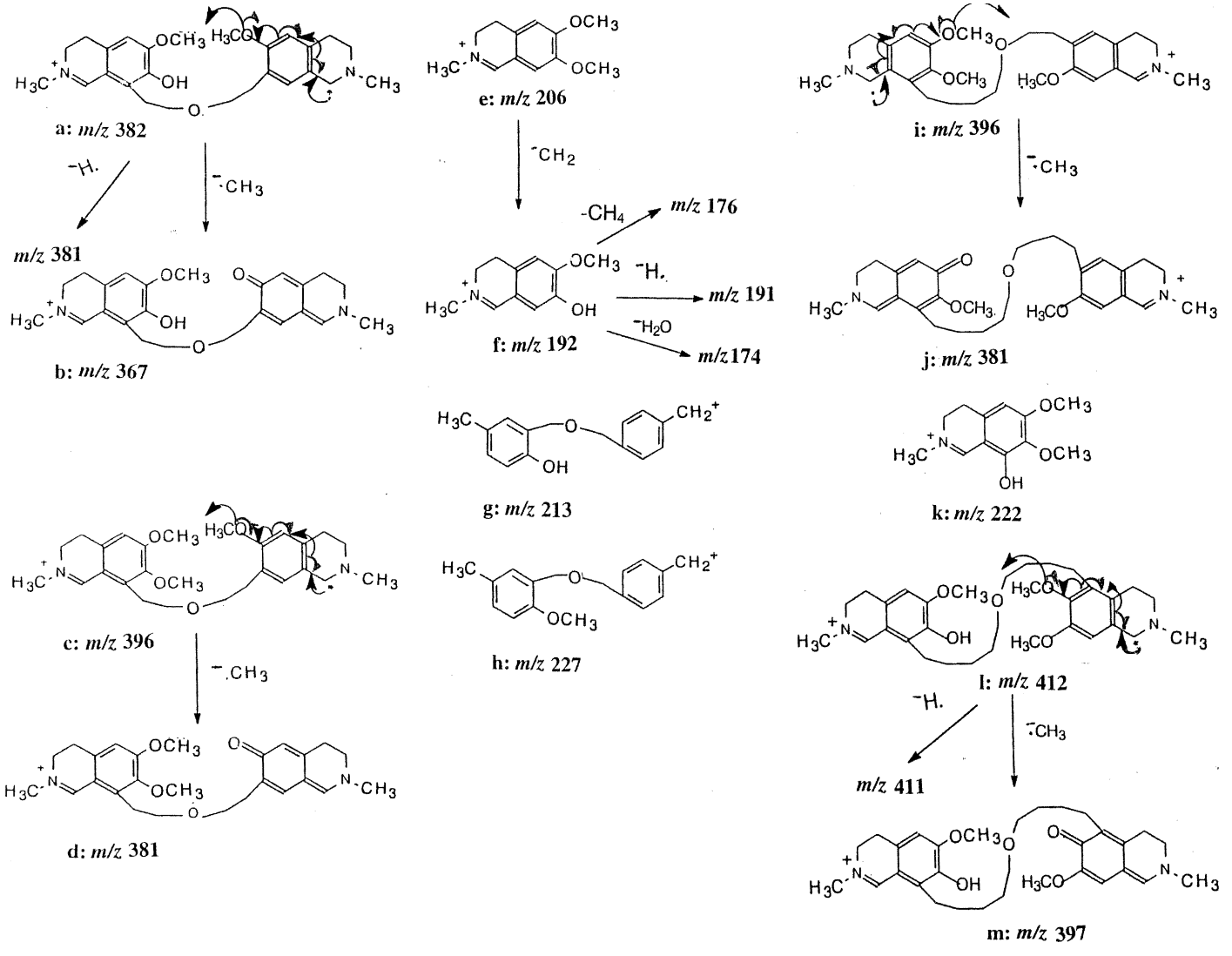

Fig. 6. Important MS/MS product ions of bisbenzylisoquinoline alkaloids.

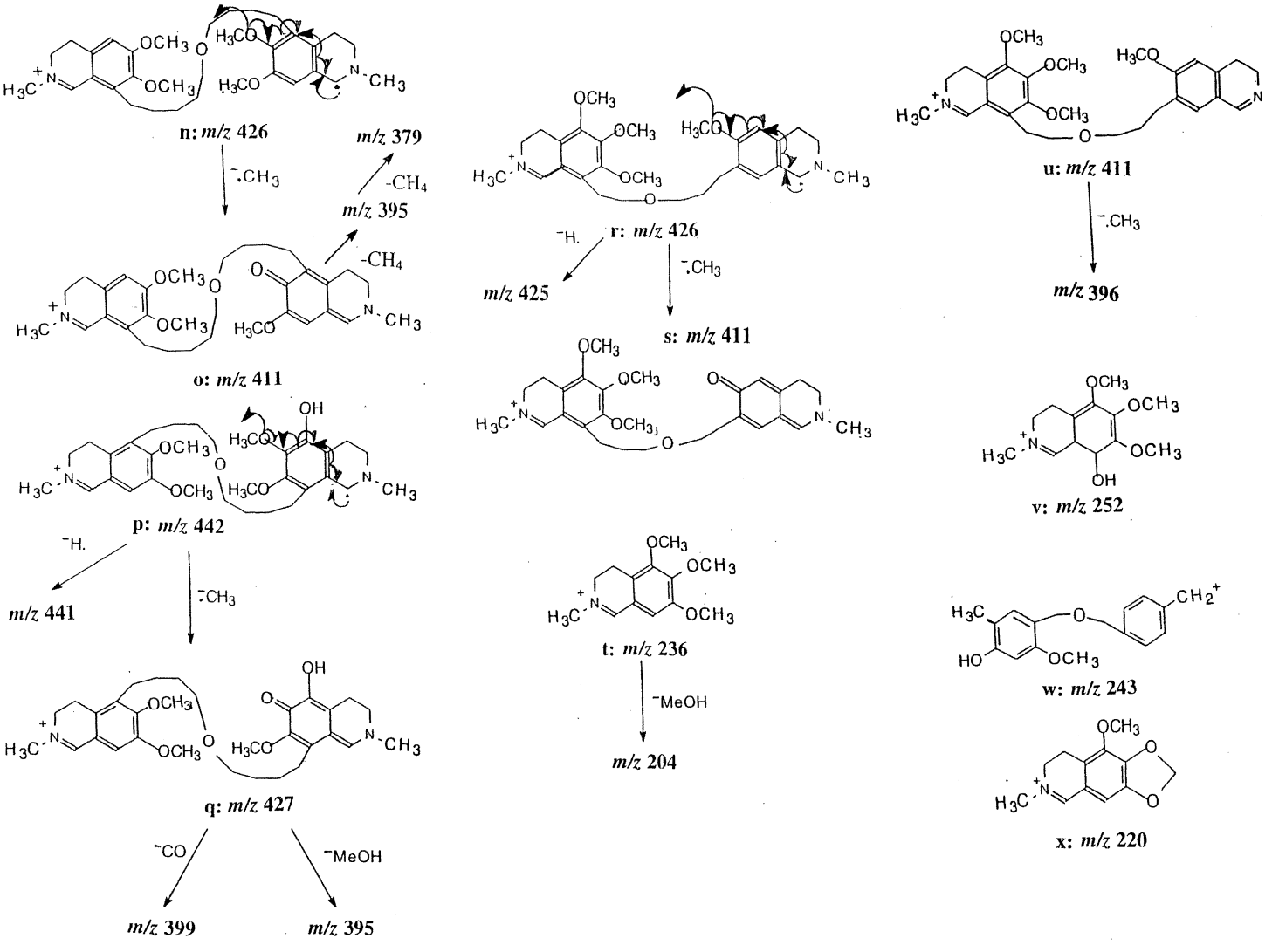

Fig. 6. (*Continued*).

Q1 scan MS. The MS/MS data provided significant product ions at *m/z* (%, r.a.) 592 ($[M + H]^+$-OMe, 31), 549 (9), 401 (65), 396 (**i**, 24), 381 (**j**, 30), 365 (**j**-CH_4, 12), 294 (11), 227 (**h**, 13), 222 (**k**, 15), 206 (**e**, 27), 192 (**f**, 10), 190 (29), 176 (**f**-CH_4, 42), 174 (**f**-H_2O, 26), and 159 (30), together with a very intense protonated molecular ion at *m/z* 623 (100) (Fig. 6).

Northalrugosidine (Fig. 1; compound #9), $C_{37}H_{40}O_7N_2$ (MW: 624), revealed a protonated molecular ion at *m/z* 625 (15%, r.a.) and an intense doubly-protonated molecular ion at *m/z* 313 (100%, r.a.) in the Q1 scan MS and the prominent product ions at *m/z* 608 ($[M + H]^+$-NH_3, 2), 594 (8), 562 (11), 398 (**l** desN-CH_3, 4), 397 (398-H, 23), 383 (398-Me, 89), 367 (383-CH_4, 79), 355 (4), 352 (367-Me, 14), 227 (**h**, 35), 222 (**k**, 18), 206 (**e**, 34), 192 (**f**, 100),190 (**f**-2H, 32), and 178 (20) with a protonated molecular ion at *m/z* 625 (13) in the MS/MS spectrum (Fig. 6).

Thalrugosidine (Fig. 1; compound #10), $C_{38}H_{42}O_7N_2$ (MW: 638), gave an apparent protonated molecular ion at *m/z* 639 (17%, r.a.) and an intense doubly-protonated molecular ion at *m/z* 320 (100%, r.a.) in the Q1 scan MS, and the structural-informative product ions at *m/z* (%, r.a.) 608 ($[M + H]^+$-OMe, 7), 576 (608-MeOH, 12), 412 (**l**, 4), 411 (**l**-H, 3), 397 (**m**,100), 381 (**m**-CH_4, 17), 368 (14), 350 (7), 227 (**h**, 8), 206 (**e**, 38), 192 (**f**, 44), 190 (**f**-2H, 27), 176 (**f**-CH_4, 8), 174 (**f**-H_2O, 9), and 159 (4), along with a protonated molecular ion at *m/z* 639 (26) in the MS/MS data (Fig. 6).

Thalidasine (Fig. 1; compound #11), $C_{39}H_{44}O_7N_2$ (MW: 652), revealed an apparent protonated molecular ion at *m/z* 653 (29%, r.a.) with a very intense doubly-protonated molecular ion at *m/z* 327 (100%, r.a.) in the MS spectrum, and the prominent product ions at *m/z* (%, r.a.) 637 ($[M + H]^+$-CH_4, 4), 622 ($[M + H]^+$-OMe, 15), 607 (622-Me, 33), 590 (607-NH_3, 28), 576 (607-OMe, 37), 560 (576-CH_4, 25), 426 (**n**, 3), 425 (**n**-H, 4), 411 (**o**, 93), 395 (411-CH_4, 20), 379 (411-MeOH, 34), 365 (395-OCH_2, 47), 227 (**h**, 24), 222 (**k**, 12), 220 (**k**-2H, 20), 206 (**e**, 100), 204 (**e**-2H, 87), 192 (**f**, 32), 190 (**e**-CH_4, 73), 174 (**e**-MeOH, 52), and 159 (22) with a protonated molecular ion at *m/z* 653 (30) in the MS/MS spectrum (Figs. 3 and 6).

Thalmirabine (compound #12), $C_{39}H_{44}O_8N_2$ (MW: 668), showed a protonated molecular ion at *m/z* 669 (23%, r.a.) with an intense doubly-protonated molecular ion at *m/z* 335 (100%, r.a.), and the MS/MS analysis provided the important fragment ions at *m/z* (%, r.a.) 653 ($[M + H]^+$-CH_4, 3), 638 ($[M + H]^+$-OMe, 13), 626 (8), 608 (14), 592 (18), 442 (**p**, 5), 441 (**p**-H, 4), 427 (**q**, 89), 410 (17), 399 (**q**-CO, 11), 395 (**q**-MeOH, 41), 380 (24), 227 (**h**, 34), 222 (**k**, 89), 220 (**k**-2H, 83), 206 (**e**, 100), 192 (**f**, 38), 190 (**f**-2H, 42), and 175 (14), with a protonated molecular ion at *m/z* 669 (23) (Fig. 6).

Thalidezine (Fig. 1; compound #13), $C_{38}H_{42}O_7N_2$ (MW: 638), showed an apparent protonated molecular ion at *m/z* 639 (10%, r.a.) and an intense doubly-protonated molecular ion at *m/z* 320 (100%, r.a.) in the Q1 scan MS spectrum, and the MS/MS spectrum indicated the structural-diagnostic product ions at *m/z* (%, r.a.) 621 ($[M + H]^+$-H_2O, 2), 608 ($[M + H]^+$-OMe, 4), 582 (3), 412 (**r** *O*-desMe, 4), 411 (**r**-H, 3), 397 (412-CH_3, 100), 395 (13), 382 (397-Me, 4), 369 (397-CO, 3), 227 (**h**, 3), 222 (**k**, 3), 206 (**e**, 5), 192 (**f**, 28), 191 (**f**-H, 40), 190 (**f**-2H, 18), and 174 (**e**-MeOH, 23), together with a protonated molecular ion at *m/z* 639 (8) (Fig. 6).

Hernandezine (Fig. 1; compound #14), $C_{39}H_{44}O_7N_2$ (MW: 652), displayed an apparent protonated molecular ion at *m/z* 653 (76%, r.a.), together with an intense doubly-protonated molecular ion at *m/z* 327 (100%, r.a.) in the MS spectrum, and the MS/MS spectrum revealed the structural-informative fragment ions at *m/z* (%, r.a.) 637 ($[M + H]^+$-CH_4, 3), 622 ($[M + H]^+$-OMe, 36), 610 (16), 595 (10), 590 (8), 426 (**r**, 7), 425 (**r**-H, 4), 411 (**s**, 100), 410 (**s**-H, 9), 395 (7), 236 (**t**, 8), 227 (**h**, 8), 204 (20), 192 (**f**, 64), 191 (**f**-H, 94), 190 (**f**-2H, 37), 176 (**f**-CH4, 18), 174 (**f**-H_2O, 27), and 162 (25) with a protonated molecular ion at *m/z* 653 (8) (Fig. 6).

Thalrugosaminine (Fig. 1; compound #15), $C_{39}H_{44}O_7N_2$ (MW: 652), exhibited an apparent protonated molecular ion at *m/z* 653 (28%, r.a.) with an intense doubly-protonated molecular ion at *m/z* 327 (100%, r.a.) in the Q1 scan MS data, and the important fragment ions at *m/z* (%, r.a.) 622 ($[M + H]^+$-OMe, 8), 591 (12), 578 (14), 426 (**r**, 3), 425 (**r**-H, 3), 411 (**s**, 81), 400 (21), 395 (18), 384 (14), 236 (**t**, 17), 227 (**h**, 26), 204 (**t**-MeOH, 68), 192 (**f**, 100), 190 (**f**-2H, 44), 176 (**f**-CH_4, 40), and 174 (**f**-H_2O, 41) accompanying with a protonated molecular ion at *m/z* 653 (29) (Figs. 4 and 6).

Thalsimine (Fig. 1; compound #16), $C_{38}H_{40}O_7N_2$ (MW: 636), showed a protonated molecular ion at *m/z* 637 (29%, r.a.) with a very intense doubly-protonated molecular ion at *m/z* 319 (100%, r.a.) in the MS spectrum, and the MS/MS spectrum displayed the prominent product ions at *m/z* (%, r.a.) 621 ($[M+H]^+$-CH_4, 18), 607 ($[M+H]^+$-CH_2O, 93), 591 (607-CH_4, 44), 576 ($[M+H]^+$-MeOH-CHO,100), 564 (27), 548 (19), 416 (18), 411 (**u**, 2), 402 (21), 396 (**u**-Me, 10), 386 (30), 370 (21), 358 (8), 265 (26), 252 (**v**, 24), 238 (**v**-CH_2, 12), 236 (**t**, 11), 227 (**h**, 5) 222 (11), 220 (**t**-CH_4, 15), 204 (**t**-MeOH, 34), 188 (8), and 176 (4) with a protonated molecular ion at *m/z* 637 (30) (Fig. 6).

Thalbrunine (Fig. 1; compound #17), $C_{39}H_{44}O_8N_2$ (MW: 668), gave a protonated molecular ion at *m/z* 669 (18%, r.a.) with an intense doubly-protonated molecular ion at *m/z* 335 (100%, r.a.) in the Q1 scan MS data, and the significant fragment ions at *m/z* (%, r.a.) 653 ($[M+H]^+$-CH_4, 3), 638 ($[M+H]^+$-OMe, 4), 426 (**r**, 8), 425 (**r**-H, 7), 411 (**s**, 100), 394 (**r**-MeOH, 21), 383 (9), 380 (13), 366 (394-CO, 34), 340 (40), 325 (23), 281 (37), 257 (13), 243 (**w**, 16), 236 (**t**, 36), 234 (**t**-2H, 34), 220 (**t**-CH_4, 40), 206 (**e**, 34), 204 (**t**-MeOH, 83), 192 (**f**, 56), 174 (**f**-H_2O, 13), and162 (32), together with a protonated molecular ion at *m/z* 669 (19) (Fig. 6).

Neothalibrine (Fig. 1; compound #18), $C_{38}H_{44}O_7N_2$ (MW: 624), revealed a weak protonated molecular ion at *m/z* 625 (1%, r.a.) and an intense doubly-protonated molecular ion at *m/z* 313 (100%, r.a.) in the MS spectrum, and the MS/MS data gave the structure-informative product ions at *m/z* (%, r.a.) 607 ($[M+H]^+$-H_2O, 1), 594 ($[M+H]^+$-OMe, 2), 432 (2), 418 (7), 402 (3), 227 (**h**, 4), 206 (**e**, 14), 192 (**f**, 100), and 177 (**f**-Me, 10), together with a protonated molecular ion at *m/z* 625 (4) (Figs. 5 and 6).

Northalistyline (Fig. 1; compound #19), $C_{40}H_{46}O_8N_2$ (MW: 682), exhibited an apparent protonated molecular ion at *m/z* 683 (2%, r.a.), along with an intense doubly-protonated molecular ion at *m/z* 342 (100%, r.a.) in the Q1 MS spectrum, and the MS/MS analysis displayed the structure-diagnostic fragment ions at *m/z* (%, r.a.) 652 ($[M+H]^+$-MeO, 4), 447 (3), 432 (7), 401 (3), 236 (**t**, 100), 227 (**h**, 5), 220 (**x**, 30), 206 (**x**-CH_2, 8), and 195 (6) with a protonated molecular ion at *m/z* 683 (4) (Fig. 6).

Thalistyline (Fig. 1; compound #20), $C_{41}H_{49}O_8N_2$ (MW: 697), displayed a weak molecular ion at *m/z* 697 (4%, r.a.), along with an intense doubly-protonated ion at *m/z* 349 (100%, r.a.), and the structural-informative fragment ions at *m/z* 666 (M^+-OMe, 3), 652 (666-CH_2, 87), 477 (7), 463 (6), 415 (13), 403 (14), 388 (12), 326 (29), 280 (35), 250 (27), 236 (**t**, 27), 227 (**h**, 10), 220 (**x**, 100), 203 (**x**-NH_3, 65), 188 (**x**-MeOH, 35), and 173 (45) with a weak molecular ion at *m/z* 697 (2) (Fig. 6).

The API-ionspray MS data of 20 bisbenzylisoquinoline alkaloids displayed intense protonated molecular ions for the 17 diether-linked compounds (#1–17), but weak protonated molecular (compounds #18 and 19) and molecular (compound #20, semi-quaternary) ions for three monoether-linked compounds, and very intense doubly-protonated molecular ions (base peak) for all compounds except thalicberine.

The MS/MS analysis of all alkaloids exhibited abundant as well as structure-diagnostic product ions via doubly-benzylic cleavages of the two benzyltetrahydroisoquinoline units. Isotetrandrine, obaberine and *O*-methyl thalicberine showed important dimeric isoquinoline fragment ions, ions **c** and **i** (*m/z* 396), and ions **d** and **j** (*m/z* 381) via the loss of a methyl from ions **c** and **i**, respectively, and both ion **e** (*m/z* 206) and ion **f** (*m/z* 192) were from isoquinoline moieties, and fragment ion **h** (*m/z* 227) was from a diphenyl ether moiety. Obamegine, thalrugosine, and homoaromoline produced the similar fragment ions as described above, ions **a** (*m/z* 382), **b** (ion **a**-Me, *m/z* 367), **e** (*m/z* 206), **f** (*m/z* 192), **g** (*m/z* 213) and **h** (*m/z* 227) (Fig. 6). Thalidasine exhibited MS/MS dimeric isoquinoline ions **n** (*m/z* 426), **o** (ion **n**-Me, *m/z* 411) as well as thalrugosidine revealed ion **l** (*m/z* 412), along with ions **h** (*m/z* 227). Thalmirabine showed MS/MS fragment ions, dimeric-isoquinoline ions **p** (*m/z* 442) and **q** (ion **p**-Me, *m/z* 427), along with ion **h** (*m/z* 227). Hernandezine, thalrugosaminine, and thalibrunine revealed MS/MS product ions, ion **r** (*m/z* 426) and ion **s** (**r**-Me, *m/z* 411), together with ion **h** (*m/z* 227) for hernandezine and thalrugosaminine, and ion **w** (*m/z* 243) for thalibrunine (Fig. 6). Thalsimine produced ion **u** (*m/z* 411), an *N*-desmethyl-iminium ion in MS/MS data (Fig. 6). Neothalibrine, a monoether-linked alkaloid, formed a major fragment ion **f** (*m/z* 192, base peak) and a minor ion **e** (*m/z* 206) (Fig. 2). While both northalistyline and thalistyline exhibited two main fragment ions, **t** (*m/z* 236) and **x** (*m/z* 220), along with ion **h** (*m/z* 227) (Fig. 6).

4. Conclusion

A total of 20 bisbenzylisoquinoline alkaloids have been investigated for MS fragmentation patterns using API-ionspray MS and MS/MS techniques. In the Q1 scan MS data, all of alkaloids revealed apparent protonated molecular or molecular (thalistyline, semi-quaternary) ions, together with very intense doubly-protonated molecular ions (base peak), which were not observed for those in the EI-MS, CI-MS [4–7,15–21] and FAB-MS [13,14]. In the API-ionspray MS/MS, the bond-cleavages between both benzylic ring E and ring AB, and ring F and ring CD formed abundant ethereal diisoquinoline ions for the most of investigated alkaloids, such as ions **a** and **b** via obamegine, thalrugosine, and homoaromoline, ions **c** and **d** via isotetrandrine, oxyacathine, and obaberine, ions **I** and **j** via thalicberine and *O*-methylthalicberine, ions **l** and **m** via thalrugosidine, ions **n** and **o** via thalidasine, ions **p** and **q** via thalmirabine, ions **r** and **s** via hernandezine, thalrugosaminine, and thalibrunine, and ion **u** via thalsimine (Fig. 6), which were similar to the fragment patterns of EI-MS, however, most of fragment ions did not observe or showed in low abundances in both CI and FAB-MS. The isoquinoline ions, such as ions **e**, **f**, **k**, **t**, **v** and **x** (Fig. 6), showed as prominent as well as intense in API-ionspray MS/MS, but revealed less abundant in EI-MS and FAB-MS These fragment ions corresponding to ethereal ring E and ring F via dibenzylic cleavages of the dimeric alkaloids, such as product ion at *m*/*z* 213 (**g**) via obamegine, oxyacathine and thalicberine, product ion at *m*/*z* 227 (**h**) via thalrugosine, isotetrandrine, obaberine, *O*-methylthalicberine, northalrugosine, thalrugosidine and thalidasine, and product ion at *m*/*z* 243 (**w**) via thalibrunine, were less abundant in the MS/MS data of all investigated alkaloids due to less ionic characteristics of these ions (Fig. 6), however, these diphenyl ether ions did not reveal in EI-MS, CI-MS and FAB-MS [1,2,4,6–21]. API-ionspray MS and MS/MS analysis of the investigated alkaloids exhibited more sensitivity of detection in Q1 scan MS and more fragment as well as intense product ions in MS/MS in nanogram quantities than those of CI-MS, EI-MS and FAB-MS in more than 10 μg quantities. In general, API-ionspray MS and MS/MS analysis is a unique technique to provide the prominent as well as diagnostic fragment ions in small quantities of materials for the structural elucidation of bisbenzylisoquinoline alkaloids as well as other alkaloids, such as quinoline, indole, and tropane alkaloids, etc.

References

[1] M. Shamma, The Isoquinoline Alkaloids-Chemistry And Pharmacology, Academic Press, New York/London, 1972, pp. 115–150.
[2] M. Shamma, L. Moniot, Isoquinoline Alkaloids Research 1972–1977, Plenum Press, New York, 1978, pp. 71–100.
[3] L.A. Mitscher, R.P. Leu, M.S. Bathala, W.N. Wu, J.L. Beal, J. Nat. Prod. 35 (1972) 157–166.
[4] P.L. Schiff Jr., J. Nat. Prod. 46 (1983) 1–43.
[5] G.A. Cordell, The Alkaloids-Chemistry and Biology, Academic Press, New York, 1998, pp. 257–311.
[6] J. Baldas, Q.N. Porter, I.R.C. Bick, M.J. Vernenge, Tetrahedron Lett. 19 (1966) 2059–2064.
[7] D.C. DeJongh, S.R. Ghrader, M.P. Cava, J. Am. Chem. Soc. 88 (1966) 1052–1055.
[8] Z.F. Ismailov ZF, S.Y. Yunusov, Khim. Prir. Soedin. 4 (1968) 256–257.
[9] J. Baldas, I.R.C. Bick, T. Ibuka, R.S. Kapil, Q.N. Porter, J.C.S., Perkin Trans. I (1972) 592–596.
[10] J. Baldas, I.R.C. Bick, M.R. Falco, J.X. DeVries, Q.N. Porter, J.C.S., Perkin Trans. I (1972) 597–601.
[11] P. Bel, A. Mandelbaum, Org. Mass Spectrom. 15 (1980) 568–572.
[12] J.L. Cashaw, S. Ruchirawart, N.Y. Somsak, E.V. Davis, Biomed. Mass Spectrom. 11 (1980) 63–67.
[13] K.P. Madhusudanan, P.R. Das, B.N. Pramanik, S. Jain, D.S. Bhakuni, Biomed. Environ. Mass Spectrom. 18 (1989) 783–790.
[14] G.W. Caldwell, J.A. Masucci, W.N. Wu, Org. Mass Spectrom. 29 (1994) 220–225.
[15] L.A. Mitscher, W.N. Wu, R.W. Doskotch, J.L. Beal, J.C.S., Chem. Comm. (1971) 589–590.
[16] W.N. Wu, J.L. Beal, R.W. Doskotch, Tetrahedron Lett. 41 (1976) 3687–3688.
[17] W.N. Wu, J.L. Beal, R.P. Leu, R.W. Doskotch, J. Nat. Prod. 40 (1977) 281–289.
[18] W.N. Wu, J.L. Beal, R.P. Leu, R.W. Doskotch, J. Nat. Prod. 40 (1977) 384–394.
[19] W.N. Wu, J.L. Beal, E.H. Fairchild, R.W. Doskotch, J. Org. Chem. 43 (1978) 580–585.
[20] W.N. Wu, J.L. Beal, R.W. Doskotch, J. Nat. Prod. 43 (1980) 372–381.
[21] J. Wu, J.L. Beal, R.W. Doskotch, J. Org. Chem. 45 (1980) 208–212.
[22] S.S. Lee, W.N. Wu, J.H. Wilton, J.L. Beal, R.W. Doskotch, J. Nat. Prod. 62 (1999) 1410–1414.
[23] W.N. Wu, M.D. Moyer, in: Proceedings of the 43rd ASMS Conference on Mass Spectrometry and Allied Topics, Atlanta, Georgia, USA, 1995, p. 526.